

J/Ψ SUPPRESSION IN AN EQUILIBRIUM HADRON GAS* **

DARIUSZ PROROK

Institute of Theoretical Physics, University of Wrocław
Pl. Maksa Born'a 9, 50-204 Wrocław, Poland

(Received March 28, 2002)

A model for J/Ψ suppression at a high energy heavy ion collision is presented. The main (and the only) reason for the suppression is J/Ψ inelastic scattering within hadron matter. The hadron matter is in the form of an evolving multi-component point-like non-interacting gas. The estimations of the sound velocity in the gas and the approximate pattern of cooling caused by the longitudinal expansion are also presented. It is shown that under such circumstances and with J/Ψ disintegration in nuclear matter added, J/Ψ suppression evaluated agrees well with NA38 and NA50 data. Additionally, some rough estimations of J/Ψ suppression in hadron matter described in the framework of the excluded volume gas model are given.

PACS numbers: 14.40.Lb, 24.10.Pa, 25.75.-q

1. Introduction

The existence of the so-called Quark–Gluon Plasma (QGP) has been the one of the most intriguing questions of high energy physics for almost two past decades. This novel state of matter has been predicted upon lattice QCD calculations (for a review see [2] and references therein) and the critical temperature T_c for the ordinary hadron matter — QGP phase transition has been estimated in the range of 150–270 MeV (this corresponds to the broad range of the critical energy density $\varepsilon_c \simeq 0.26\text{--}5.5$ GeV/fm³). Since NA50 Collaboration estimates for the energy density obtained in the Central Rapidity Region (CRR) give the value of 3.5 GeV/fm³ for the most central Pb–Pb data point [3], it is argued that the region of the existence of the QGP has been reached in Pb–Pb collisions at CERN SPS. The main argument for

* Presented at the Cracow Epiphany Conference on Quarks and Gluons in Extreme Conditions, Cracow, Poland, January 3–6, 2002.

** Talk based on the work done in collaboration with L. Turko [1].

the QGP creation during Pb–Pb collisions at the CERN SPS is the observation of the suppression of J/Ψ relative yield. J/Ψ suppression as a signal for the QGP formation was originally proposed by Matsui and Satz [4]. The clue point of the NA50 Collaboration paper [3] is the figure (denoted as Fig. 6 there), where experimental data for Pb–Pb collision values of $B_{\mu\mu}\sigma_{J/\psi}/\sigma_{\text{DY}}$ (the ratio of the J/Ψ to the Drell–Yan production cross-section times the branching ratio of the J/Ψ into a muon pair) are presented together with some conventional predictions. Here, “conventional” means that J/Ψ suppression is due to J/Ψ absorption in ordinary hadron matter. Since all those conventional curves saturate at high transverse energy E_T , but the experimental data fall from $E_T \simeq 90$ GeV much lower and this behavior could be reproduced on the base of J/Ψ disintegration in QGP [5], it is argued that QGP had to appear during most central Pb–Pb collisions. In general, the immediate reservation about such reasoning is that besides those already known (see *e.g.* [6–10] and references [12–15] in [3]), there could be a huge number of different conventional models, so until this subject is cleared up completely, it is not legitimate to rule out the absorption picture of J/Ψ suppression.

In the following talk, the more systematic and general description of J/Ψ absorption in the framework of statistical analysis will be presented. The main features of the model are [1]:

1. A multi-component non-interacting hadron gas appears in the CRR instead of the QGP.
2. The gas expands longitudinally and transversely.
3. J/Ψ suppression is the result of inelastic scattering on constituents of the gas and on nucleons of colliding ions.

2. The timetable of events in the CRR

For a given A – B collision $t = 0$ is fixed at the moment of the maximal overlap of the nuclei (for more details see *e.g.* [9]). As nuclei pass each other charmonium states are produced as the result of gluon fusion. After half of the time the nuclei need to cross each other ($t \sim 0.5$ fm), matter appears in the CRR. It is assumed that the matter thermalizes almost immediately and the moment of thermalization, t_0 , is estimated at about 1 fm [9, 11]. Then the matter begins its expansion and cooling and after reaching the freeze-out temperature, $T_{\text{f.o.}}$, it ceases as a thermodynamical system. The moment when the temperature has decreased to $T_{\text{f.o.}}$ is denoted as $t_{\text{f.o.}}$. Since the matter under consideration is the hadron gas, no phase transition takes place during cooling here.

For the description of the evolution of the matter, relativistic hydrodynamic is explored. The longitudinal component of the solution of hydrodynamic equations (the exact analytic solution for an (1+1)-dimensional case) reads (for details see *e.g.* [11, 12])

$$s(\tau) = \frac{s_0 \tau_0}{\tau}, \quad n_B(\tau) = \frac{n_B^0 \tau_0}{\tau}, \quad v_z = \frac{z}{t}, \quad (1)$$

where $\tau = \sqrt{t^2 - z^2}$ is a local proper time, v_z is the z -component of fluid velocity (z is a collision axis) and s_0 and n_B^0 are initial densities of the entropy and the baryon number, respectively. For $n_B = 0$ and the uniform initial temperature distribution with the sharp edge at the border established by nuclei radii, the full solution of (3+1)-dimensional hydrodynamic equations is known [13]. The evolution derived is the decomposition of the longitudinal expansion inside a slice bordered by the front of the rarefaction wave and the transverse expansion which is superimposed outside of the wave. Because small but nevertheless non-zero baryon number densities are considered here, the above mentioned description of the evolution has to be treated as an assumption in the presented model. The rarefaction wave moves radially inward with a sound velocity c_s (see Sec. 4).

3. The multi-component hadron gas

For an ideal hadron gas in thermal and chemical equilibrium, which consists of l species of particles (here, mesons are up to K_2^* and baryons up to Ω^-), energy density ε , baryon number density n_B , strangeness density n_S and entropy density s read ($\hbar = c = 1$ always)

$$\varepsilon = \frac{1}{2\pi^2} \sum_{i=1}^l (2s_i + 1) \int_0^\infty dp \frac{p^2 E_i}{\exp\left\{\frac{E_i - \mu_i}{T}\right\} + g_i}, \quad (2a)$$

$$n_B = \frac{1}{2\pi^2} \sum_{i=1}^l (2s_i + 1) \int_0^\infty dp \frac{p^2 B_i}{\exp\left\{\frac{E_i - \mu_i}{T}\right\} + g_i}, \quad (2b)$$

$$n_S = \frac{1}{2\pi^2} \sum_{i=1}^l (2s_i + 1) \int_0^\infty dp \frac{p^2 S_i}{\exp\left\{\frac{E_i - \mu_i}{T}\right\} + g_i}, \quad (2c)$$

$$s = \frac{1}{6\pi^2 T^2} \sum_{i=1}^l (2s_i + 1) \int_0^\infty dp \frac{p^4}{E_i} \frac{(E_i - \mu_i) \exp\left\{\frac{E_i - \mu_i}{T}\right\}}{\left(\exp\left\{\frac{E_i - \mu_i}{T}\right\} + g_i\right)^2}, \quad (2d)$$

where $E_i = (m_i^2 + p^2)^{1/2}$ and m_i , B_i , S_i , μ_i , s_i and g_i are the mass, baryon number, strangeness, chemical potential, spin and a statistical factor of specie i , respectively (an antiparticle is treated as a different specie). And $\mu_i = B_i\mu_B + S_i\mu_S$, where μ_B and μ_S are overall baryon number and strangeness chemical potentials, respectively.

To obtain the time dependence of temperature and baryon number and strangeness chemical potentials one has to solve numerically equations (2b)–(2d) with s , n_B and n_S given as time dependent quantities. For $s(\tau)$ and $n_B(\tau)$ expressions (1) are taken and $n_S = 0$ since the overall strangeness equals zero during all the evolution (see Sec. 5).

4. The sound velocity in the multi-component hadron gas

In the hadron gas the sound velocity squared is given by the standard expression

$$c_s^2 = \frac{\partial P}{\partial \varepsilon}. \quad (3)$$

Since the experimental data for heavy-ion collisions suggests that the baryon number density is non-zero in the CRR at AGS and SPS energies [14–16], we calculate the above derivative for various values of n_B [17, 18].

To estimate initial baryon number density n_B^0 we can use experimental results for S–S [14] or Au–Au [15, 16] collisions. In the first approximation we can assume that the baryon multiplicity per unit rapidity in the CRR is proportional to the number of participating nucleons. For a sulphur–sulphur collision we have $dN_B/dy \cong 6$ [14] and 64 participating nucleons. For the central collision of lead nuclei we can estimate the number of participating nucleons at $2A = 416$, so we have $dN_B/dy \cong 39$. Having taken the initial volume in the CRR equal to $\pi R_A^2 \times 1$ fm, we arrive at $n_B^0 \cong 0.25$ fm⁻³. This is some underestimation because the S–S collisions were at a beam energy of 200 GeV/nucleon, but Pb–Pb at 158 GeV/nucleon. From the Au–Au data extrapolation one can estimate $n_B^0 \cong 0.65$ fm⁻³ [15]. These values are for central collisions. So, we estimate (3) for $n_B = 0.25$, 0.65 fm⁻³ and additionally, to investigate the dependence on n_B much carefully, for $n_B = 0.05$ fm⁻³. The results of numerical evaluations of (3) are presented in Fig. 1. For comparison, we drew also two additional curves: for $n_B = 0$ and for a pure massive pion gas. These curves are taken from [17].

The “physical region” lies between more or less 100 and 200 MeV on the temperature axis. This is because the critical temperature for the possible QGP-hadronic matter transition is of the order of 200 MeV [2] and the freeze-out temperature should not be lower than 100 MeV [15]. In low temperatures we can see completely different behaviors of cases with $n_B = 0$ and $n_B \neq 0$.

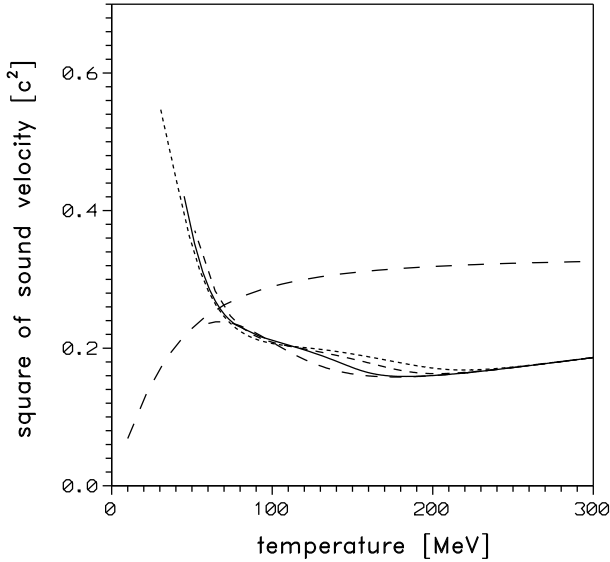


Fig. 1. Dependence of the sound velocity squared on temperature for various values of n_B : $n_B = 0.65 \text{ fm}^{-3}$ (short-dashed), $n_B = 0.25 \text{ fm}^{-3}$ (dashed), $n_B = 0.05 \text{ fm}^{-3}$ (solid) and $n_B = 0$ (long-dashed). The case of the pure pion gas (extra-long-dashed) is also presented.

We think that this is caused by the fact that for $n_B \neq 0$ the gas density cannot reach zero when $T \rightarrow 0$, whereas for $n_B = 0$ it can. For the higher temperatures all curves excluding the pion case behave in the same way qualitatively. From $T \approx 70$ MeV they decrease to their minima (for $n_B = 0.65 \text{ fm}^{-3}$ at $T \cong 219.6$ MeV, for $n_B = 0.25 \text{ fm}^{-3}$ at $T \cong 202.5$ MeV, for $n_B = 0.05 \text{ fm}^{-3}$ at $T \cong 183.4$ MeV and for $n_B = 0$ at $T \cong 177.3$ MeV) and then they increase to cover each other above $T \approx 250$ MeV.

To compare with the more realistic picture, we also calculated the sound velocity for the excluded volume multi-component hadron gas model (for details of the model see [19]). The gas consists of the same species of particles as in Sec. 3. The radii of all particles are assumed to be the same and equal to 0.4 fm [20]. The results are presented in Fig. 2. The most crucial new feature of the sound velocity is that it can be greater than 1 in some wide intervals of temperature. This has already been noticed [21], but for the case with baryon number and strangeness chemical potentials equal to zero. Note that now there is strong dependence of the sound velocity on the baryon number density, only cases with $n_B = 0.0, 0.05 \text{ fm}^{-3}$ have c_s^2 values comparable with the case of the point-like gas in the “physical region” (*cf.* Fig. 1 and Fig. 2).

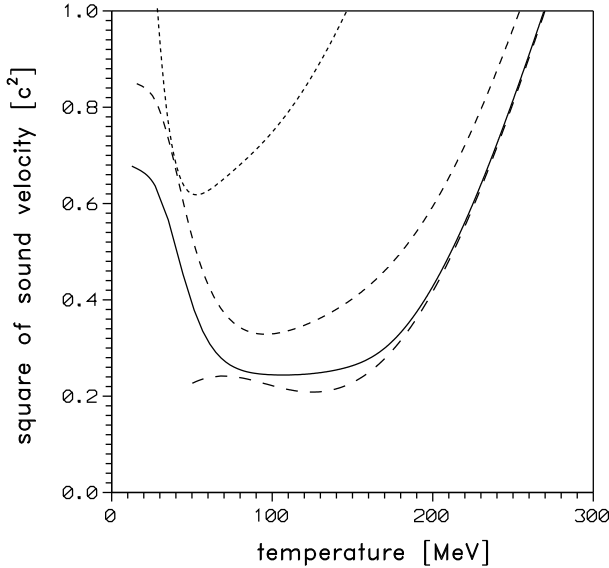


Fig. 2. Dependence of the sound velocity squared on temperature for the excluded volume hadron gas model for various values of n_B : $n_B = 0.65 \text{ fm}^{-3}$ (short-dashed), $n_B = 0.25 \text{ fm}^{-3}$ (dashed), $n_B = 0.05 \text{ fm}^{-3}$ (solid) and $n_B = 0$ (long-dashed).

5. The pattern of cooling and its connection with the sound velocity

In Sec. 3 we have explained how to obtain the time dependence of the temperature of the longitudinally expanding hadron gas. This dependence proved to be very well approximated by the expression [17, 18]

$$T(\tau) \cong T_0 \tau^{-a}. \quad (4)$$

The above approximation is valid in the temperature ranges $[T_{f.o.}, T_0]$, where $T_{f.o.} \geq 100 \text{ MeV}$, $T_0 \leq T_{0,\text{max}}$ and $T_{0,\text{max}} \approx 230 \text{ MeV}$. We started from T_0 equal to 227.2 MeV (for $n_B^0 = 0.65 \text{ fm}^{-3}$), 229.3 MeV (for $n_B^0 = 0.25 \text{ fm}^{-3}$) and 229.7 MeV (for $n_B^0 = 0.05 \text{ fm}^{-3}$). These values correspond to $\varepsilon_0 = 5.0 \text{ GeV/fm}^3$ (the initial energy density in the CRR has been estimated by NA50 [3] at $\varepsilon_0 = 3.5 \text{ GeV/fm}^3$). Then we took several decreasing values of $T_0 < T_{0,\text{max}}$. For every T_0 chosen we repeat the procedure of obtaining the approximation (4), *i.e.* the power a . The values of a as a function of T_0 are depicted in Fig. 3 for the case of $n_B = 0.25 \text{ fm}^{-3}$, together with the corresponding sound velocity curve. We can see that in the above mentioned interval of temperature the power a has the meaning of the sound velocity squared within quite well accuracy. We would like to stress that we arrived at the same conclusion also for cases with $n_B = 0.65 \text{ fm}^{-3}$ and $n_B = 0.05 \text{ fm}^{-3}$.

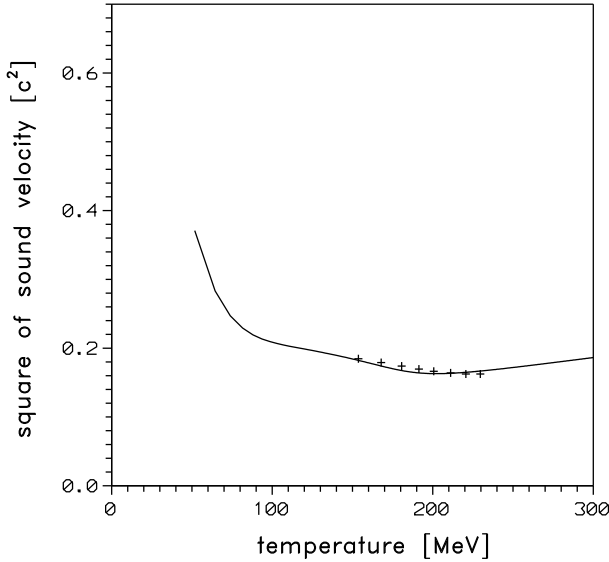


Fig. 3. The power a (crosses) from the approximation (4) and the sound velocity curve for $n_B = 0.25 \text{ fm}^{-3}$.

We can formulate the following conclusion: in the “physical region” of temperature and for realistic baryon number densities, the longitudinal expansion given by (1) results in the cooling of the hadron gas described by (4) with $a = c_s^2(T_0)$, namely:

$$T(\tau) \cong T_0 \left(\frac{\tau_0}{\tau} \right) c_s^2(T_0) \tag{5}$$

where T_0 belongs to the “physical region”. Note that $T(\tau) = T_0 \left(\frac{\tau_0}{\tau} \right) c_s^2$ is the exact expression for a baryon-less gas with the sound velocity constant (for details see [12, 13]). It should be stressed that c_s^2 in (5) is constant only for the particular cooling from a given T_0 . For different T_0 the value of c_s^2 in (5) will change appropriately, that is to the value of c_s^2 in the hadron gas with the temperature equal to this new T_0 . The approximation (5) will be used to simplify evaluations of J/Ψ survival factors in the next sections.

It should be added that for the excluded volume hadron gas model the above mentioned conclusion is no longer valid. We did the appropriate simulations, but approximations of $T(\tau)$ by a power function were much worse and values of the power obtained were a factor 2 lower than the square of the velocity of sound.

6. J/Ψ absorption in the expanding hadronic gas

As it has been already mentioned in Sec. 2 charmonium states are produced in the beginning of the collision, when nuclei overlap. For simplicity, it is assumed that the production of $c\bar{c}$ states takes place at $t = 0$. To describe J/Ψ absorption quantitatively, the idea of [9] is generalized to the case of the multi-component massive gas, here. Since in the CRR longitudinal momenta of particles are much lower than transverse ones (in the c.m.s. frame of nuclei), J/Ψ longitudinal momentum is put at zero. Additionally, only the plane $z = 0$ is under consideration, here. For the simplicity of the model, it is assumed that all charmonium states are completely formed and can be absorbed by the constituents of a surrounding medium from the moment of creation. The absorption is the result of a $c\bar{c}$ state inelastic scattering on the constituents of the hadron gas through interactions of the type

$$c\bar{c} + h \longrightarrow D + \bar{D} + X, \quad (6)$$

where h denotes a hadron, D is a charm meson and X means a particle which is necessary to conserve the charge, baryon number or strangeness.

Since the most crucial for the problem of QGP existence are Pb–Pb collisions (see remarks in Sec. 1), the further considerations are done for this case. So, for the Pb–Pb collision at impact parameter b , the situation in the plane $z = 0$ is presented in Fig. 4, where S_{eff} means the area of the overlap of the colliding nuclei.

Additionally, it is assumed that the hadron gas, which appears in the space between the nuclei after they have crossed each other, also has the shape of S_{eff} at t_0 in the plane $z = 0$. Then, the transverse expansion starts in the form of the rarefaction wave moving inward S_{eff} at t_0 .

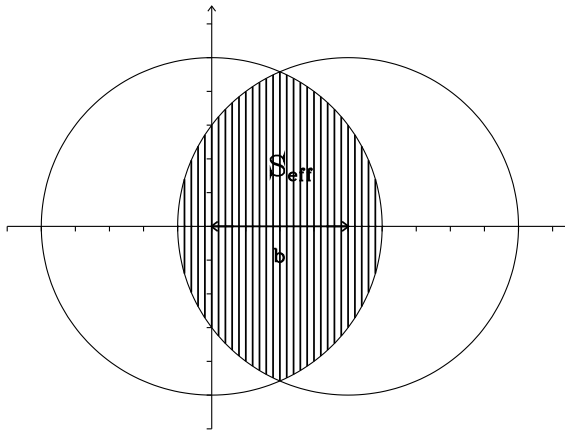


Fig. 4. View of a Pb–Pb collision at impact parameter b in the transverse plane ($z = 0$). The region where the nuclei overlap is hatched and denoted by S_{eff} .

From the considerations based on the relativistic kinetic equation (for details see [1,9]), the survival fraction of *J/Ψ* in the hadron gas as a function of the initial energy density ε_0 in the CRR is obtained:

$$\mathcal{N}_{\text{h.g.}}(\varepsilon_0) = \int dp_T g(p_T, \varepsilon_0) \times \exp \left\{ - \int_{t_0}^{t_{\text{final}}} dt \sum_{i=1}^l \int \frac{d^3 \vec{q}}{(2\pi)^3} f_i(\vec{q}, t) \sigma_i v_{\text{rel},i} \frac{p_\nu q_i^\nu}{E E_i'} \right\}, \quad (7)$$

where the sum is over all taken species of scatters (hadrons), $p^\nu = (E, \vec{p}_T)$ and $q_i^\nu = (E_i', \vec{q})$ are four momenta of *J/Ψ* and hadron specie *i*, respectively, σ_i states for the absorption cross-section of *J/Ψ* – *h_i* scattering, $v_{\text{rel},i}$ is the relative velocity of *h_i* hadron with respect to *J/Ψ* and *M* and *m_i* denote *J/Ψ* and *h_i* masses, respectively (*M* = 3097 MeV). The function $g(p_T, \varepsilon_0)$ is the *J/Ψ* initial momentum distribution. It has a gaussian form and reflects gluon multiple elastic scatterings on nucleons before their fusion into a *J/Ψ* in the first stage of the collision [22–25]. The upper limit of the integration over time in (7), namely t_{final} is the minimal value of $\langle t_{\text{esc}} \rangle$ and $t_{\text{f.o.}}$. The quantity $\langle t_{\text{esc}} \rangle$ is the average time of the escape of *J/Ψ*'s from the hadron medium for given values of *b* and *J/Ψ* velocity $\vec{v} = \vec{p}_T/E$. Note that the average is taken with the weight

$$p_{J/\Psi}(\vec{r}) = \frac{T_A(\vec{r}) T_B(\vec{r} - \vec{b})}{T_{AB}(b)}, \quad (8)$$

where $T_{AB}(b) = \int d^2 \vec{s} T_A(\vec{s}) T_B(\vec{s} - \vec{b})$, $T_A(\vec{s}) = \int dz \rho_A(\vec{s}, z)$ and $\rho_A(\vec{s}, z)$ is the nuclear matter density distribution. For the last quantity, the Woods–Saxon nuclear matter density distribution with parameters from [26] is taken. In the integration over hadron momentum in (7) the threshold for the reaction (6) is included, *i.e.* σ_i equals zero for $(p^\nu + q_i^\nu)^2 < (2m_D + m_X)^2$ and is constant elsewhere (m_D is a charm meson mass, $m_D = 1867$ MeV). Also the usual Bose–Einstein or Fermi–Dirac distribution for hadron specie *i* is used in (7)

$$f_i(\vec{q}, t) = f_i(q, t) = \frac{2s_i + 1}{\exp \left\{ \frac{E_i' - \mu_i(t)}{T(t)} \right\} + g_i}. \quad (9)$$

For simplicity, we use (5) as the approximation to $T(t)$ in (9) and $\mu_B(t)$ and $\mu_S(t)$ are solutions of only two equations (2b), (2c) with T given by (5), $n_B(t)$ by (1) and $n_S(t) = 0$.

As far as σ_i is concerned, there are no data for every particular J/Ψ - h_i scattering. Therefore, only two types of the cross-section, the first, σ_b , for J/Ψ -baryon scattering and the second, σ_m , for J/Ψ -meson scattering are assumed, here. In the model presented σ_b is put at $\sigma_{J/\psi N}$ — J/Ψ -nucleon absorption cross-section. And values of $\sigma_{J/\psi N}$ in the range of 3–5 mb are taken from p - A data [27–29]. The J/Ψ -meson cross-section σ_m is assumed to be 2/3 of σ_b , which is due to the quark counting.

As it has been already suggested [27] also J/Ψ scattering in nuclear matter should be included in any J/Ψ absorption model. This could be done with the introduction of J/Ψ survival factor in nuclear matter [29–32]

$$\mathcal{N}_{\text{n.m.}}(\varepsilon_0) \cong \exp \left\{ -\sigma_{J/\psi N} \rho_0 L \right\} , \quad (10)$$

where ρ_0 is the nuclear matter density and L the mean path length of the J/Ψ through the colliding nuclei. The length L is expressed by the following formula [32]:

$$\rho_0 L(b) = \frac{1}{2T_{AB}} \int d^2 \vec{s} T_A(\vec{s}) T_B(\vec{s} - \vec{b}) \left[\frac{A-1}{A} T_A(\vec{s}) + \frac{B-1}{B} T_B(\vec{s} - \vec{b}) \right] . \quad (11)$$

Since J/Ψ absorptions: in nuclear matter and in the hadron gas, are separate in time, J/Ψ survival factor for a heavy-ion collision with the initial energy density ε_0 , could be defined as

$$\mathcal{N}(\varepsilon_0) = \mathcal{N}_{\text{n.m.}}(\varepsilon_0) \mathcal{N}_{\text{h.g.}}(\varepsilon_0) . \quad (12)$$

Note that since right sides of (7) and (10) include parts which depend on impact parameter b and the left sides are functions of ε_0 only, the expression converting the first quantity to the second (or reverse) should be given. This is done with the use of the dependence of ε_0 on the transverse energy E_T extracted from NA50 data [3] (for details see [1]).

To make the model as much realistic as possible, one should keep in mind that only about 60% of J/Ψ 's measured are directly produced during collision. The rest is the result of χ ($\sim 30\%$) and ψ' ($\sim 10\%$) decays [33]. Therefore the realistic J/Ψ survival factor could be expressed as

$$\mathcal{N}(\varepsilon_0) = 0.6 \mathcal{N}_{J/\psi}(\varepsilon_0) + 0.3 \mathcal{N}_\chi(\varepsilon_0) + 0.1 \mathcal{N}_{\psi'}(\varepsilon_0) , \quad (13)$$

where $\mathcal{N}_{J/\psi}(\varepsilon_0)$, $\mathcal{N}_\chi(\varepsilon_0)$ and $\mathcal{N}_{\psi'}(\varepsilon_0)$ are given also by formulae (7), (10) and (12) but with $g(p_T, \varepsilon_0)$, $\sigma_{J/\psi N}$ and M changed appropriately (for details see [1]).

To complete, also values of cross-sections for χ -baryon and ψ' -baryon scatterings are needed. For simplicity, it is assumed that both these cross-sections are equal to J/Ψ -baryon one. Since J/Ψ is smaller than χ or ψ' , this means that J/Ψ suppression evaluated according to (13) is *underestimated* here.

7. Results

Now we can complete calculations of formula (7) for values of n_B^0 given in Sec. 4. The last parameter of the model is the freeze-out temperature. Two values $T_{f.o.} = 100, 140$ MeV are taken here and they agree well with estimates based on hadron yields [15].

Firstly, formula (13) with the use of (7) only instead of (12) is calculated for the case of (1+1)-dimensional expansion and results are presented in Figs. 5, 6.

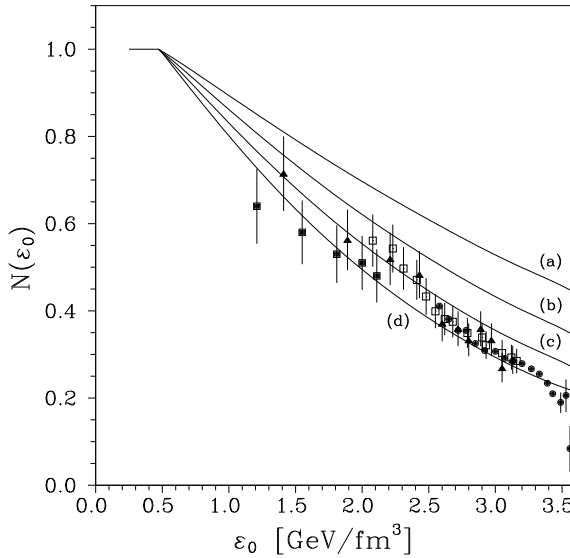


Fig. 5. *J/ψ* suppression in the longitudinally expanding hadron gas for $n_B^0 = 0.25 \text{ fm}^{-3}$ and $T_{f.o.} = 140$ MeV: (a) $\sigma_b = 3$ mb, $\sigma_m = 2$ mb; (b) $\sigma_b = 4$ mb, $\sigma_m = 2.66$ mb; (c) $\sigma_b = 5$ mb, $\sigma_m = 3.33$ mb; (d) $\sigma_b = 6$ mb, $\sigma_m = 4$ mb. The black squares correspond to the NA38 S-U data [34], the black triangles correspond to the 1996 NA50 Pb-Pb data, the white squares to the 1996 analysis with minimum bias and the black points to the 1998 analysis with minimum bias [3].

For comparison, also the experimental data are shown in Figs. 5, 6. The experimental survival factor is defined as

$$\mathcal{N}_{\text{exp}} = \frac{\frac{B_{\mu\mu}\sigma_{J/\psi}^{AB}}{\sigma_{DY}^{AB}}}{\frac{B_{\mu\mu}\sigma_{J/\psi}^{pp}}{\sigma_{DY}^{pp}}}, \tag{14}$$

where $B_{\mu\mu}\sigma_{J/\psi}^{AB(pp)}/\sigma_{\text{DY}}^{AB(pp)}$ is the ratio of the J/Ψ to the Drell–Yan production cross-section in A – B (p – p) interactions times the branching ratio of the J/Ψ into a muon pair. The values of the ratio for p – p , S–U and Pb–Pb are taken from [3,34,35]. The results of numerical evaluations of (13) agree well with the data qualitatively for greater baryonic cross-section σ_b and (or) for the lower freeze-out temperature $T_{\text{f.o.}}$, except the last point measured for the highest E_T bin.

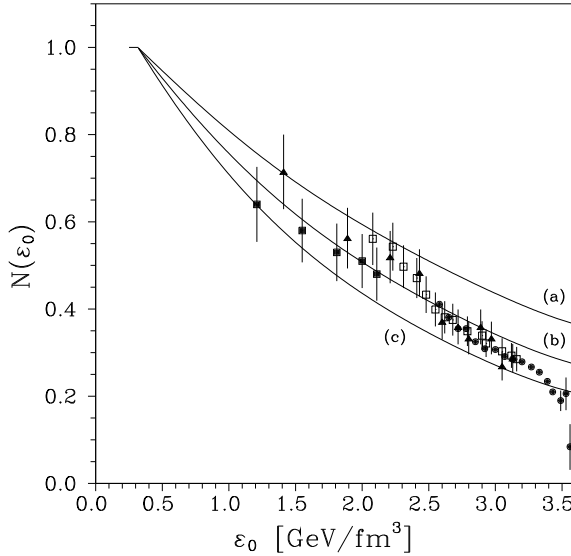


Fig. 6. Same as Fig. 2 (except case (d), which is not presented here) but for $T_{\text{f.o.}} = 100$ MeV.

Now the full (3+1)-dimensional hydrodynamic evolution (in the form described in Sec. 2) and J/Ψ absorption in nuclear matter will be taken into account and results are depicted in Figs. 7, 8. To draw also S–U data together with Pb–Pb ones, instead of multiplying $\mathcal{N}_{\text{h.g.}}$ by $\mathcal{N}_{\text{n.m.}}$, \mathcal{N}_{exp} is divided by $\mathcal{N}_{\text{n.m.}}$, *i.e.* “the experimental J/Ψ hadron gas survival factor” is defined as

$$\tilde{\mathcal{N}}_{\text{exp}} = \exp \{ \sigma_{J/\psi N} \rho_0 L \} \mathcal{N}_{\text{exp}} , \quad (15)$$

and values of this factor are drawn in Figs. 7, 8 as the experimental data. The quantity r_0 is a parameter from the expression for a nucleus radius $R_A = r_0 A^{1/3}$. The value of R_A is used to fix the initial position of the rarefaction wave in the evaluation of $\langle t_{\text{esc}} \rangle$ in (7). It has turned out that the case of $n_B^0 = 0.05 \text{ fm}^{-3}$ does not differ substantially from that of $n_B^0 = 0.25 \text{ fm}^{-3}$, so curves for $n_B^0 = 0.05 \text{ fm}^{-3}$ are not depicted in Figs. 7, 8.

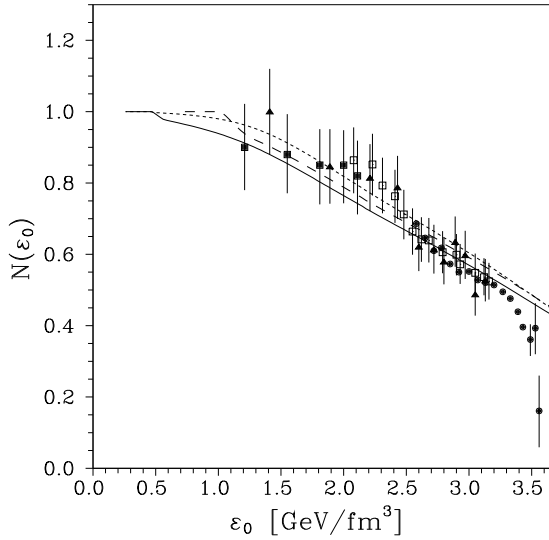


Fig. 7. *J/Ψ* suppression in the longitudinally and transversely expanding hadron gas for the Woods–Saxon nuclear matter density distribution and $\sigma_b = 4$ mb, $\sigma_m = 2.66$ mb and $T_{f.o.} = 140$ MeV. The curves correspond to $n_B^0 = 0.25$ fm $^{-3}$, $c_s = 0.45$, $r_0 = 1.2$ fm (solid), $n_B^0 = 0.65$ fm $^{-3}$, $c_s = 0.46$, $r_0 = 1.2$ fm (dashed) and $n_B^0 = 0.25$ fm $^{-3}$, $c_s = 0.45$, $r_0 = 1.12$ fm (short-dashed). The black squares represent the NA38 S–U data [34], the black triangles represent the 1996 NA50 Pb–Pb data, the white squares the 1996 analysis with minimum bias and the black points the 1998 analysis with minimum bias [3], but the data are “cleaned out” from the contribution of *J/Ψ* scattering in the nuclear matter in accordance with (15).

Having compared Figs. 7, 8 with Figs. 5, 6, one can see that adding the transverse expansion changes the final (theoretical) pattern of *J/Ψ* suppression qualitatively. Now the curves for the case including the transverse expansion are not convex, in opposite to the case with the longitudinal expansion only, where the curves are. As far as the pattern of suppression is concerned, theoretical curves do not fall steep enough at high ϵ_0 to cover the data area. But for some choice of parameters, namely for σ_b somewhere between 4 and 5 mb and for $r_0 = 1.12$ fm, a quite satisfactory curve could have been obtained. Precisely, again only the highest E_T bin point falls down of the range of theoretical estimates completely. But the error bar of this point is very wide. And also the contradiction in positions of the last three points of the 1998 data can be seen. This means that the high E_T region should be measured once more with the better accuracy to state definitely whether the abrupt fall of the experimental survival factor takes place there or not.

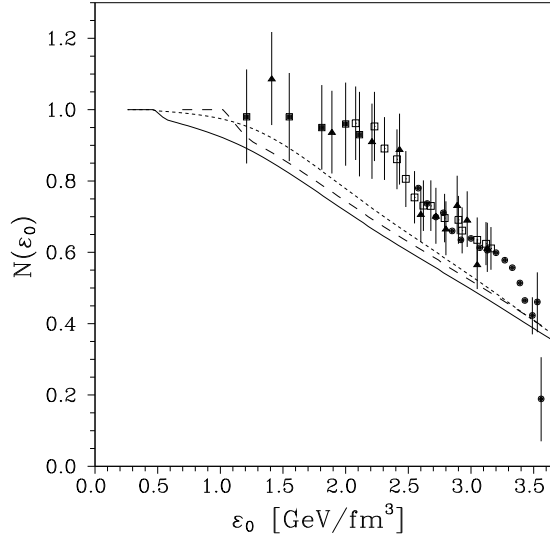


Fig. 8. Same as Fig. 7 but for $\sigma_b = 5$ mb and $\sigma_m = 3.33$ mb.

To support the conclusion, main results from Figs. 7, 8 are presented in Fig. 9 again. The original data [3] for $B_{\mu\mu}\sigma_{J/\psi}^{\text{PbPb}}/\sigma_{\text{DY}}^{\text{PbPb}}$ and J/Ψ survival factors given by (13) multiplied by $B_{\mu\mu}\sigma_{J/\psi}^{\text{pp}}/\sigma_{\text{DY}}^{\text{pp}}$ and now as functions of E_T are depicted there (for details see [1]). As it has been already mentioned, the main disagreement with the data appears in the last experimental point of the 1998 analysis.

The charmonium-baryon inelastic cross-section is the most crucial parameter in the model presented. So to be sure what is the exact result of J/Ψ absorption, one should know how this cross-section behaves in the hot hadron environment. The newest estimations of $\pi + J/\Psi$, $\rho + J/\Psi$ and $J/\Psi + N$ cross-sections at high invariant collision energies [36,37] give values of σ_b and σ_m of the same order as assumed here. Also it should be stressed that the charmonium-hadron inelastic cross-sections are considered as constant quantities in the model presented. But, as the results of just mentioned papers suggest, they are not constant at all. The cross-sections are growing functions of the invariant collision energy \sqrt{s} . Therefore, one could think naively that the increase of ε_0 (or in other words E_T) causes the increase of the invariant collision energy \sqrt{s} on the average and further the increase of the charmonium-hadron inelastic cross-sections. In this way, the line describing J/Ψ survival factor could be placed close to the solid curve of Fig. 9 for low ε_0 (E_T), and then, as the charmonium-hadron inelastic cross-sections increase, this line would go closer to the dashed curve of Fig. 9 for high ε_0 (E_T). So, the experimental pattern of J/Ψ suppression could be recovered.

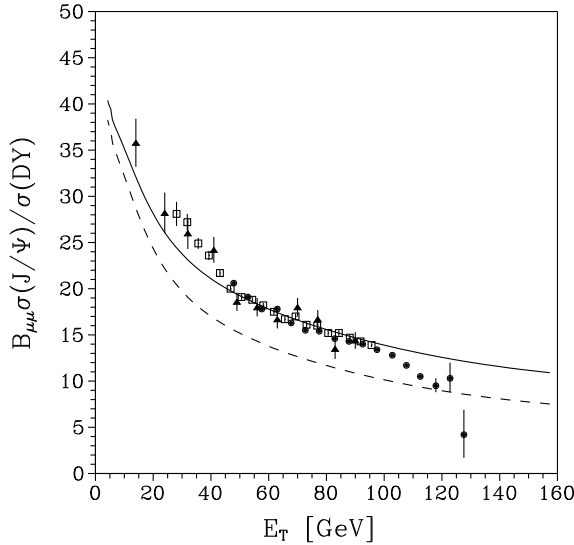


Fig. 9. *J/Ψ* survival factor times $B_{\mu\mu}\sigma_{J/\psi}^{pp}/\sigma_{DY}^{pp}$ in the longitudinally and transversely expanding hadron gas for the Woods-Saxon nuclear matter density distribution and $n_B^0 = 0.25 \text{ fm}^{-3}$, $T_{f.o.} = 140 \text{ MeV}$, $c_s = 0.45$ and $r_0 = 1.2 \text{ fm}$. The curves correspond to $\sigma_b = 4 \text{ mb}$ (solid) and $\sigma_b = 5 \text{ mb}$ (dashed). The black triangles represent the 1996 NA50 Pb-Pb data, the white squares the 1996 analysis with minimum bias and the black points the 1998 analysis with minimum bias [3].

8. The suppression in the hadron matter described by the excluded volume gas model

As a last remark an extension to the point-like gas model will be discussed. The rough estimation of *J/Ψ* suppression in the framework of the excluded volume gas model [19] will be presented now. The estimation done suggests that *J/Ψ* suppression is much lower in the gas of particles with hard core radii than in the point-like one. There are two main reasons for such behavior:

1. the freeze-out time resulting from the longitudinal expansion only, is much shorter for the excluded volume gas than for the point-like one, namely for $n_B^0 = 0.25 \text{ fm}^{-3}$, $T_{f.o.} = 140 \text{ MeV}$ and $\varepsilon_0 = 3.5 \text{ GeV/fm}^3$ one obtains $t_{f.o.}^{\text{ex.v.}} \simeq 9.4 \text{ fm}$ and $t_{f.o.}^{\text{p.l.}} \simeq 15.1 \text{ fm}$ (“ex.v.” means “excluded volume” and “p.l.” “point-like”);
2. the initial particle density is much lower for the excluded volume gas than for the point-like one, that is $n_0^{\text{ex.v.}} = 0.8 \text{ fm}^{-3}$ and $n_0^{\text{p.l.}} = 2.6 \text{ fm}^{-3}$.

To estimate how these two facts influence J/Ψ survival factor the very rough approximation to (7) is explored. If the transverse expansion, particle masses and thresholds are neglected, then (7) takes the following very simple form:

$$\mathcal{N}_{\text{h.g.}} = \exp \left\{ -\sigma n_0 t_0 \ln \frac{t_{\text{f.o.}}}{t_0} \right\}, \quad (16)$$

where σ means one common cross-section for all particles. So, for values of $t_{\text{f.o.}}^{\text{p.-l.}}$, $t_{\text{f.o.}}^{\text{ex.v.}}$ and $n_0^{\text{p.-l.}}$, $n_0^{\text{ex.v.}}$ given above and for $\sigma = \sigma_m = 3.33$ mb one obtains:

$$\mathcal{N}_{\text{h.g.}}^{\text{p.-l.}} \simeq 0.1, \quad \mathcal{N}_{\text{h.g.}}^{\text{ex.v.}} \simeq 0.6. \quad (17)$$

For comparison $\mathcal{N}_{\text{exp}} = 0.1\text{--}0.2$ there. Therefore, J/Ψ survival factor evaluated for the excluded volume gas model is far above experimentally allowed values. This means that J/Ψ suppression in a hadron gas is very much model dependent.

9. Conclusions

To sum up and to stress how vague the idea of J/Ψ suppression as a signal of QGP is, the author would like to call reader's attention to Fig. 5 of [38]. The solid and dotted curves in that figure are exactly the same as curves just presented in Fig. 9. But the distortion in the QGP is the main reason for J/Ψ suppression in [38]! It is also stated there, that results shown "provide evidence for the production of the quark-gluon plasma in central high-energy Pb-Pb collisions". So, one could say as well that the NA50 Pb-Pb data provides evidence for the production of the thermalized and *confined* hadron gas in the central rapidity region of a Pb-Pb collision. But estimations done in Sec. 8 have just shown that it could not be true.

Therefore, the final conclusion is the following: J/Ψ suppression is not a good signal for the quark-gluon plasma appearance at a central heavy-ion collision.

This work was partially supported by the Polish State Committee for Scientific Research (KBN) contract no. 2 P03B 030 18.

REFERENCES

- [1] D. Prorok, L. Turko, *Phys. Rev.* **C64**, 044903 (2001).
- [2] F. Karsch, [hep-ph/0103314](#); *Nucl. Phys. Proc. Suppl.* **83**, 14 (2000).
- [3] M.C. Abreu *et al.* (NA50 Collaboration), *Phys. Lett.* **B477**, 28 (2000).
- [4] T. Matsui, H. Satz, *Phys. Lett.* **B178**, 416 (1986).
- [5] H. Satz, *Nucl. Phys.* **A661**, 104c (1999).
- [6] J. Ftáčnik, P. Lichard, J. Pišút, *Phys. Lett.* **B207**, 194 (1988).
- [7] R. Vogt, M. Prakash, P. Koch, T.H. Hansson, *Phys. Lett.* **B207**, 263 (1988).
- [8] S. Gavin, M. Gyulassy, A. Jackson, *Phys. Lett.* **B207**, 257 (1988).
- [9] J.P. Blaizot, J.Y. Ollitrault, *Phys. Rev.* **D39**, 232 (1989).
- [10] R. Vogt, *Phys. Rep.* **310**, 197 (1999).
- [11] J.D. Bjorken, *Phys. Rev.* **D27**, 140 (1983).
- [12] J. Cleymans, R.V. Gavai, E. Suhonen, *Phys. Rep.* **130**, 217 (1986).
- [13] G. Baym, B.L. Friman, J.P. Blaizot, M. Soyeur, W. Czyż, *Nucl. Phys.* **A407**, 541 (1983).
- [14] J. Baechler *et al.* (NA35 Collaboration), *Nucl. Phys.* **A525**, 59C (1991).
- [15] J. Stachel, *Nucl. Phys.* **A654**, 119C (1999).
- [16] L. Ahle *et al.* (E802 Collaboration), *Phys. Rev.* **C57**, R466 (1998).
- [17] D. Prorok, L. Turko, *Z. Phys.* **C68**, 315 (1995).
- [18] D. Prorok, L. Turko, [hep-ph/0101220](#).
- [19] G.D. Yen, M.I. Gorenstein, W. Greiner, S.N. Yang, *Phys. Rev.* **C56**, 2210 (1997).
- [20] P. Braun-Munzinger, D. Magestro, K. Redlich, J. Stachel, *Phys. Lett.* **B518**, 41 (2001).
- [21] R. Venugopalan, M. Prakash, *Nucl. Phys.* **A546**, 718 (1992).
- [22] J. Hüfner, Y. Kurihara, H.J. Pirner, *Phys. Lett.* **B215**, 218 (1988).
- [23] S. Gavin, M. Gyulassy, *Phys. Lett.* **B214**, 241 (1988).
- [24] J.P. Blaizot, J.Y. Ollitrault, *Phys. Lett.* **B217**, 392 (1989).
- [25] S. Gupta, H. Satz, *Phys. Lett.* **B283**, 439 (1992).
- [26] C.W. de Jager, H. de Vries, C. de Vries, *At. Data Nucl. Data Tables* **14**, 479 (1974).
- [27] C. Gerschel, J. Hüfner, *Phys. Lett.* **B207**, 253 (1988).
- [28] J. Badier *et al.* (NA3 Collaboration), *Z. Phys.* **C20**, 101 (1983).
- [29] S. Gavin, R. Vogt, *Phys. Rev. Lett.* **78**, 1006 (1997).
- [30] C. Gerschel, J. Hüfner, *Z. Phys.* **C56**, 171 (1992).
- [31] S. Gavin, [hep-ph/9609470](#).
- [32] F. Bellaiche, PhD Thesis, Université Claude Bernard Lyon-I, Lyon 1997; F. Fleuret, PhD Thesis, Ecole Polytechnique, Palaiseau 1997.

- [33] H. Satz, hep-ph/9711289.
- [34] M.C. Abreu *et al.* (NA38 Collaboration), *Phys. Lett.* **B449**, 128 (1999);
M.C. Abreu *et al.*, *Phys. Lett.* **B466**, 408 (1999).
- [35] M.C. Abreu *et al.* (NA50 Collaboration), *Phys. Lett.* **B450**, 456 (1999).
- [36] K. Tsushima, A. Sibirtsev, K. Saito, A.W. Thomas, D.H. Lu, *Nucl. Phys.*
A680, 279 (2000).
- [37] A. Sibirtsev, K. Tsushima, A.W. Thomas, nucl-th/0005041.
- [38] C. Wong, *Nucl. Phys.* **A681**, 22 (2001).